

Experimental Investigation on Micro Structure and Mechanical Behavior of AA 6063 - 7075 Dissimilar joint using Activated TIG Welding

Rajiv Kumar^a, Harmesh Kumar Kansal^b, S. C. Vettivel^c

^aResearch Scholar, UIET, Panjab university, Chandigarh, India

^bProfessor, UIET, Panjab university, Chandigarh, India

^cCCET (Degree Wing), Chandigarh, India

ABSTRACT

Article Info

Publication Issue :

Volume 10, Issue 1

January-February-2023

Page Number : 16-38

Article History

Accepted : 05 Jan 2023

Published: 19 Jan 2023

This paper is mainly focused on the Activated Tungsten Inert gas welding (ATIG) characterization and mechanical behavior of AA 6063 - 7075 dissimilar joint using TiO₂ flux with the filler of AA 5356 and compared with conventional TIG. The characterization of the Base Material (BM), Fusion Zone (FZ), Heat Affected Zone (HAZ) and partially melted zone are carried out using the Optical Microscope. The quality of the weld is characterized using Ultrasonic assisted non destructive evaluation. A-Scan result confirms that the ATIG welded samples having more DOP and less bead width as compared to conventional TIG. The recorded tensile strength of conventional TIG and ATIG welded with flux (TiO₂) sample 135 and 173 MPa respectively.

Keywords: TIG welding, Activated TIG welding, Microstructure, Flux

I. INTRODUCTION

Activated Tungsten Inert Gas (ATIG) welding is a technique that can produce an enhanced weld penetration in a single pass. There are certain cases because of which the use of this technique is restricted such as inferior weld surface quality and inferior metallurgical and mechanical properties and also its use, especially in industries. Different results are obtained by performing A-TIG welding on different types of steels and fluxes provided [1]. It is

a process involving the application of a thin coating of flux over the joint area before welding and it helps in increasing the weld penetration at the same parameters than the conventional TIG welding. A summary of the effect of different types of fluxes on the different types of steels by the researchers has been discussed [2].

The phenomenon of sensitization and hot cracking are always of top-most importance while performing such a task. Welding process like limit passes, removal of filler metal and lowering the heat input

shall favour for its joining. Single oxides powders such as CaO, Al₂O₃, Cr₂O₃, TiO₂, and SiO₂ were used for this study. Due to the use of the last three oxide powder the increase in the penetration was indicated in the results [3]. A-TIG welding has shown intense enhancement in-depth penetration, reduced weld width and subsequent increase in the weld depth to width ratio as compared to the TIG process with the same parameters [4]. Deeper and narrower welds are generated in A-TIG welding than the conventional TIG welding and the coated surface also reduces the diameter of the plasma arc column [5].

AA7075 aluminum alloy with the GTA process and studied the tensile properties behavior due to the effect of pulse current and post-weld aging treatment. He used four different welding techniques to fabricate the joints with Continuous current TIG welding processes, the welded joint efficiency is much lower when it was compared with the base metal [6]. Also it was concluded that In TIG welds current pulsing leads to fine or more equiaxed grain structure. TIG welding of AA6063 aluminium alloy, there is a significant strength reduction near the

welds due to over-aging but the size of the HAZ is small (less than 10 mm). The compressive residual stresses near the fillet welds had a strong positive influence on the fatigue life [7].

Even though researchers have studied the effect of flux on mechanical behaviour on ATIG welded joints. But nobody has studied the effect on AA6063 and AA7075. In this study AA 6063 –AA7075 dissimilar alloy is used as BM. The mechanical behavior and microstructure using ATIG with TiO₂ is studied. Trials test are conducted to select welding parameters as explained in [8-10].

II. METHODS AND MATERIAL

2.1 Materials

1000*300*6 mm plate of AA6063 and AA 7075 was used as BM in this study. The composition and mechanical properties of the AA6063-T6 is listed in Table 1(a&b) and for the filler wire is presented in the Table 2.

Table 1(a) AA 6063 T6 Chemical Composition

Alloy	Al	Si	Cu	Mn	Mg	Cr	Fe	Zn
6063-T6	97.9	0.2-0.6	0.1	0.1	0.7	0.1	0.35	0.1

Table 1(b) AA 7075 T6 Chemical Composition

Alloy	Al	Si	Cu	Mn	Mg	Cr	Fe	Zn
7075 T6	91.4	0.4	1.5	0.3	2.9	0.28	0.5	6.0

Table 2 Filler Rod AA 5356 Chemical Composition

Alloy	Al	Si	Fe	Cu	Ti	Zn	Mn	Mg
AA 5356	Bal	0.25	0.40	0.10	0.20	0.10	0.10	4.5

2.1.2 Fluxes

Three ceramic oxide flux TiO_2 was used to analyze the quality of the welded joints using ATIG. The quantity of flux used per samples is $3-4 * 10^{-2} \text{ mg/mm}^2$. The oxide fluxes are purchased from Akshar Exim Company Private Limited, Kolkata, West Bengal, India. The chemical compositions of the ceramic fluxes are listed in Table 3.

Table 3 Chemical composition of ceramic fluxes

Molecular Formula	Density g/cm^3	Melting Point, $^{\circ}\text{C}$	Boiling P	Molecular Weight, g/mol
TiO_2	4.23	1855 $^{\circ}\text{C}$	2973	79.865

2.2. Methods

2.2.1 Preparation of activation mixture

The preparation of the activation mixture is one of the important tasks in ATIG welding. The mass of the flux required for a welding is calculated from the volume calculation as explained in [1-2]

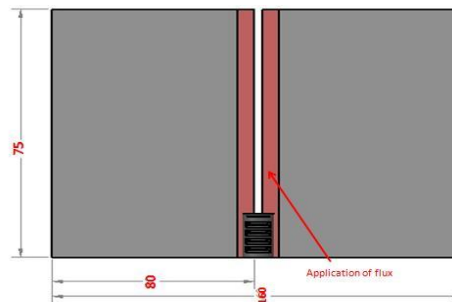


Fig. 1 Applied flux surface

2.2.2. ATIG Welding

TIG welding power source (Make: Panasonic, Model BR1-200 (AC/DC), capacity: 250 A with machine torch) with standard argon gas with regulator was used for welding. A 6 mm thick plate was cut into $160 \times 75 \text{ mm}$. The surface impurities and uneven surfaces were removed with the help of surface grinding followed by cleaning with acetone. Before welding the arc length was adjusted to 3 mm between the electrode tip and work piece. Coated tungsten electrode rod with a diameter 3 mm was used in welding. The blunt angle of electrode tip was $20-22^{\circ}$ and was positioned at 4–5 mm out of the nozzle. A homogenous mixture of ceramic fluxes was prepared with the help of acetone which was added in proportion 6–8 ml/g. After the preparation of flux mixture, it was applied just before ATIG welding as represented in Fig.1.

2.3 Mechanical test

The mechanical behaviour of the conventional TIG and ATIG were studied through tensile and hardness test. The samples were cut using wire cut Electrical Discharge Machining. The cutting was done perpendicular to the direction of the weld.

2.4 Tensile test

The tensile test was done at CITCO, Industrial Area, Chandigarh, India using FIE MAKE Universal Testing Machine. The Samples were prepared and as per ASTM E-8M standard. The data was analysed for each specimen and mean value was recorded.

2.5 Characterization

3.1 Effect of depth of penetration and quality of weld

In ATIG welding with flux TiO_2 following effects were identified. Below 160 A the DOP was very poor at the same time above 220 A burning of metal was observed. It is concluded that the full DOP without any major defects identified at 200 A.

Fig. 2 shows the DOP, Width of bead and ultra sonic A scan results of the conventional TIG and ATIG welded with flux TiO_2 at 200 A. The sectional view showing DOP of conventional TIG and ATIG with fluxes TiO_2 is shown in Fig. 2(a, d) and the effect of fluxes on bead width is shown in Fig. 2(b, e). The Fig. 2(a, b, d,) confirmed that conventional TIG welded samples had more bead width and less DOP as compared to the ATIG welded sample using flux (TiO_2). This is mainly due to the gradient of surface tension at outer periphery is very high as compared to centre of weld pool. The excess amount of oxygen from the fluxes increase the heat input as a result DOP increased [13]. Fig. 2 (c&f) shows A scan result of the conventional TIG welding and ATIG respectively. The recorded DOP is 4.8 mm and bead width is 17 mm as shown in Fig. 2(a & b). and Fig. 2(d & e) for ATIG is 6 mm and width 9 mm respectively. It confirmed that there is gain in DOP with flux TiO_2 . It confirms the DOP is not up to the full depth. Fig. 2(f) shows the NDE A scan result of the A TIG welding with flux TiO_2

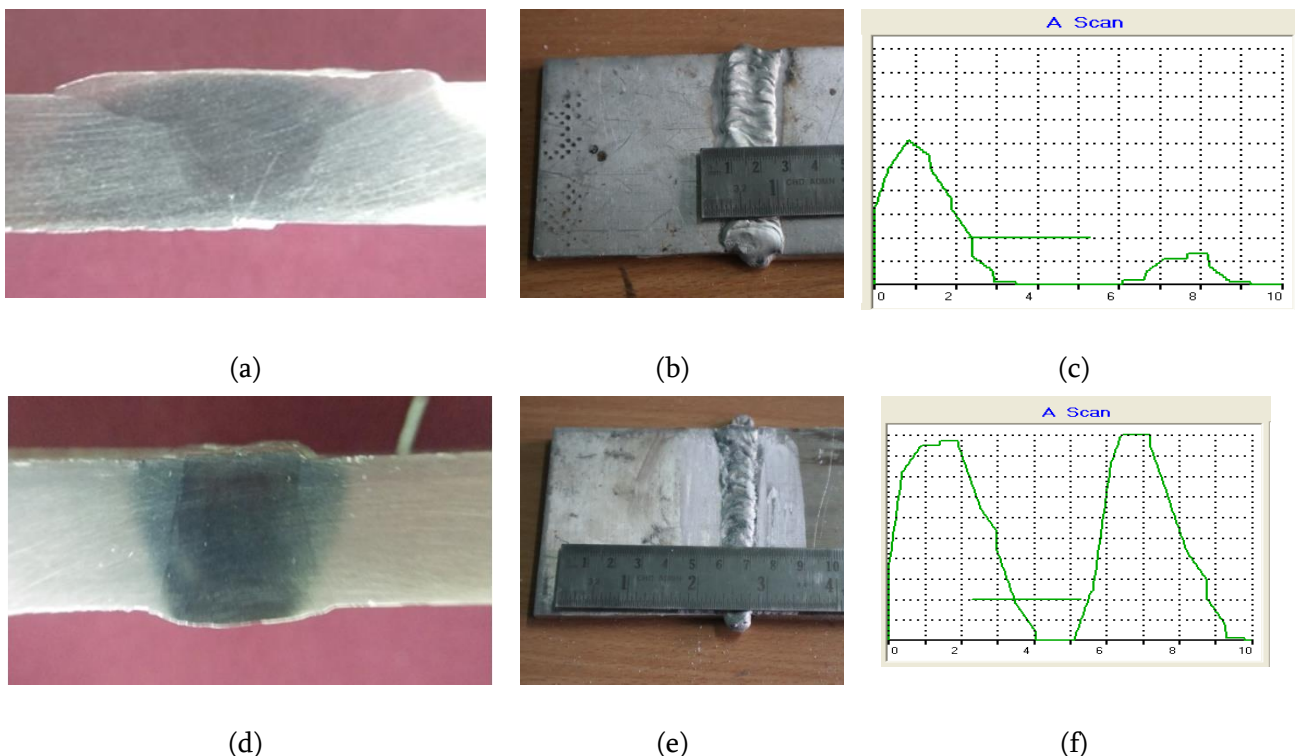


Fig.2 DOP, Bead width and ultrasonic A scan of conventional TIG and ATIG welded samples (a) DOP of conventional TIG (b) width of conventional TIG (c) A scan of conventional TIG (d) DOP of ATIG using TiO_2 (e) width of ATIG using TiO_2 (f) A scan of ATIG using TiO_2

2.5.1 Optical microscope

The samples have been prepared by using mounting press and polished with the help different grit size varied from 50 to 3000. Paste of alumina and diamond along with the velvet cloth is used to smooth the surface of the specimen at Chandigarh College of Engineering Technology (Degree Wing), Chandigarh, India. The samples were etched with Keller's reagent after polishing to view the microstructure with help of the Optical Microscope (RADICAL, model RXM 7).

3.2.1 OM Characterization

The weldments for conventional TIG and ATIG using flux TiO_2 can be divided into three sections as FZ, HAZ and PMZ regions which are observed in Fig. 3(b, c). The classification of these regions is done on the basis of the temperature attained at the time of welding. The BM AA7075-T6 microstructure contain insoluble phases and the secondary phases like Mg_2Zn and Al_2CuMg , $MgAl_3$, and Mg_2Si . The grains in the BM are elongated from centre towards fusion line.

In Fig. 3(b & d), it was observed that FZ of each sample contains shows the weld region which consists of long dendrites of the primary and secondary phases. The secondary phase shows Al-Si particles and it is recorded that FZ has fine inter dendritic network of Al-Si particles.

Fig. 3 (a, b, c & d.) are the microstructure of BM, HAZ, PMZ & FZ. It is observed while comparing BM and HAZ grain structure that the BM contains precipitation hardened matrix. The HAZ shows secondary phases Al-Si which is resulted from primary phase of aluminium. It is also confirmed at the interface grain flow vanished. The grains solidify towards the fusion line as the temperature gradient is aligned in the direction of weld pool. The random disorientation between grains of BM and weldment is shown in Fig. 3(b & c) [11].

The PMZ is the region of the HAZ where temperature crossed the equilibrium solidus limit [12]. The microstructures revealed that BM and HAZ have more long dendrites of the primary and secondary phases as compared to the PMZ. Hence, PMZ is weakest area. Therefore, the failures will occur at PMZ. This is confirmed by tensile test.

Fig. 3(b & d) confirm the microstructure in ATIG with TiO_2 is finer as compared to the conventional TIG joints. This is mainly due to spacing in the dendrite arms. Also the dendrite arm spacing in ATIG is less as compared to conventional TIG welded joints.

Fig. 3(b & c) shows the microstructure varies towards the centre FZ from the fusion line. The size of grains in HAZ of conventional TIG is more as compared to ATIG with TiO_2 . Also the high temperature exposure precipitates $ZnAl_2$ and Mg_2Si phases and coarsen the grains which resulted in the softening of HAZ [13].

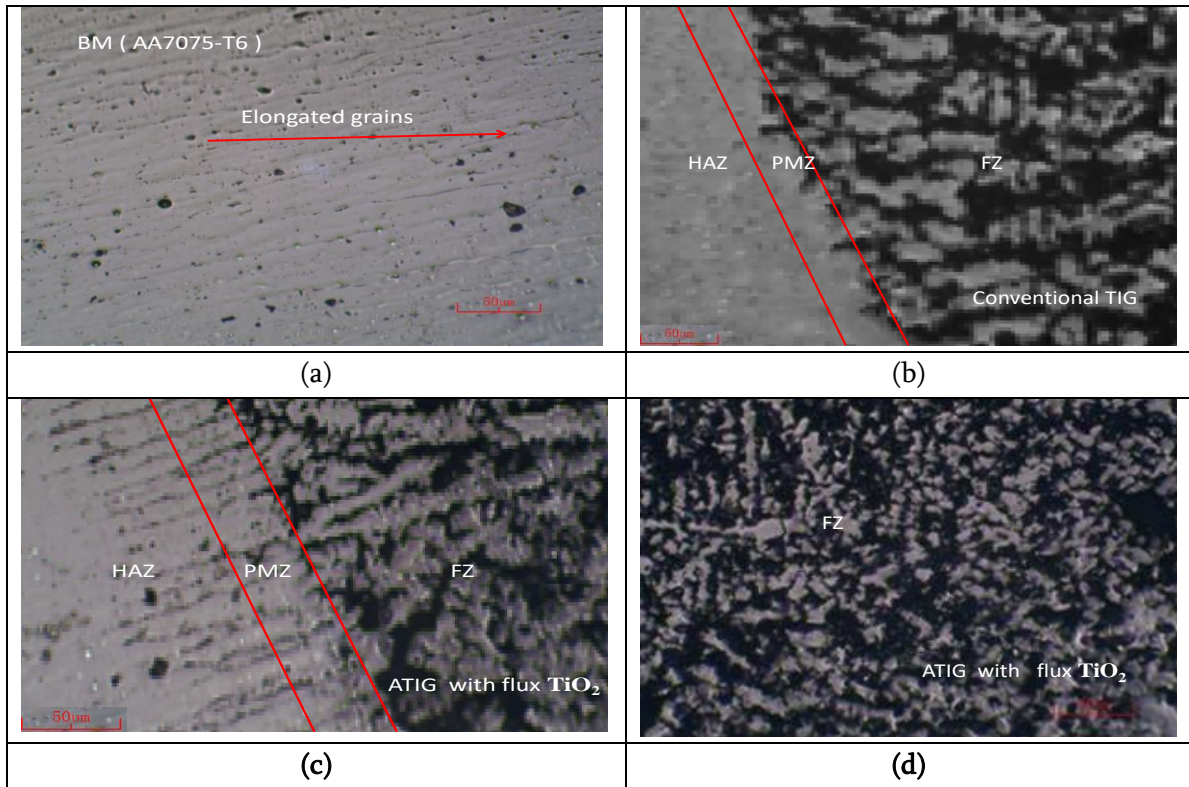
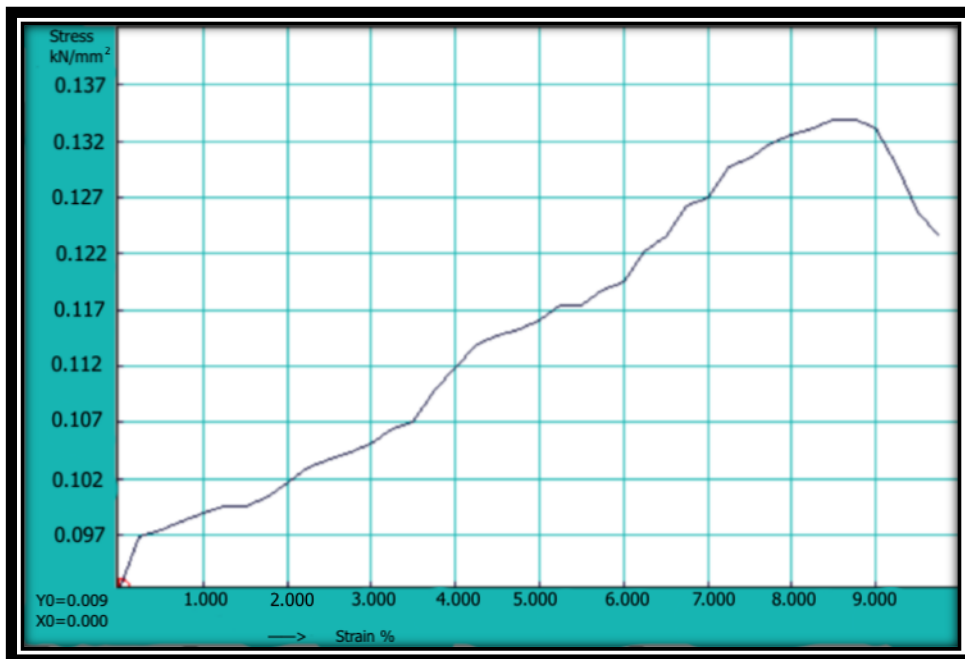


Fig. 3 OM characterization of conventional TIG and ATIG with flux TiO₂ (a) BM (b) FZ of conventional TIG (c) ATIG using TiO₂ (d) FZ of ATIG using TiO₂

III. Results and Discussion

3.1 Effect of tensile strength and micro structure

It is confirmed from Fig. 3 the tensile strength of ATIG with flux TiO₂ along with filler rod AA5356 is 172 MPa. Also it is confirmed that the tensile strength of the ATIG welded joint is more as compared to conventional TIG [1].



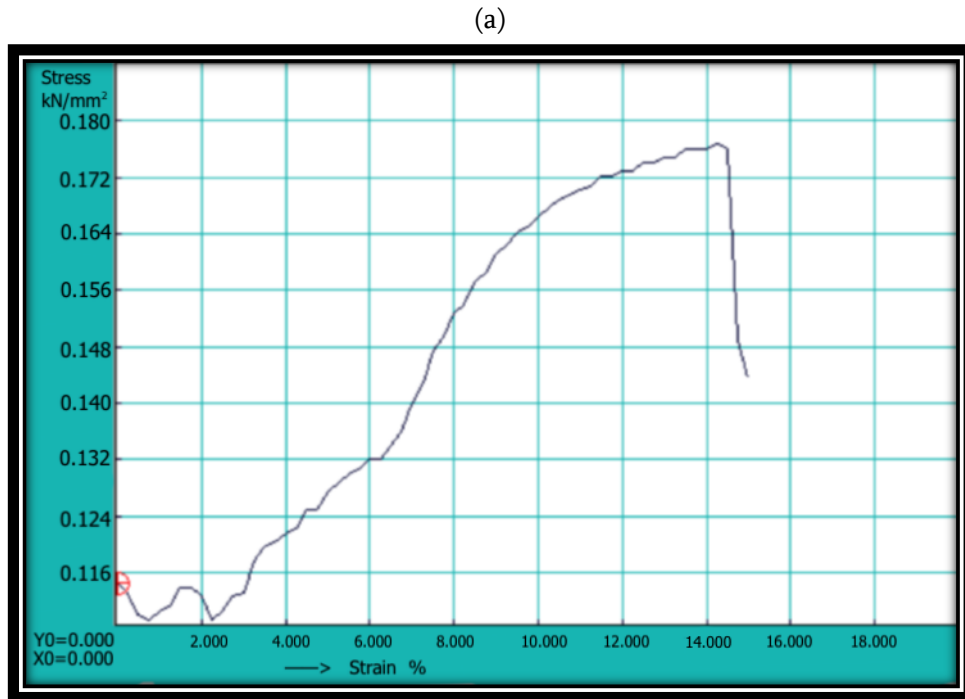


Fig. 3 Effect of tensile strength (a) Conventional TIG (b) ATIG using TiO₂ flux

IV. CONCLUSION

ATIG welding with ceramic flux TiO₂ of AA6063-AA7075 with filler AA 5356 were carried out at optimum gas flow rate. The influence of ceramic fluxes TiO₂, on the microstructure, and mechanical properties were studied and the following conclusions are drawn:

- The ceramic fluxes in ATIG welding increased the DOP and decreased the bead width
- The recorded tensile strength of ATIG with flux TiO₂ is 172 MPa.

V. REFERENCES

[1]. Rajiv Kumar, SC Vettivel, Harmesh Kumar Kansal, "Effect of SiO₂ flux on the depth of penetration, microstructure, texture and mechanical behavior of AA6063 T6 aluminum

alloy using activated TIG welding" Bulletin of the Polish Academy of Sciences: Technical Sciences, Vol. 69(1), 2021, pages 1-8, Article number: e136215 DOI: 10.24425/bpasts.2020.136215.

- [2]. H. Li, J. Zou, J. Yao, H. Peng, The effect of TIG welding techniques on microstructure, properties and porosity of the welded joint of 2219 aluminum alloy, J. Alloys Compd. 727 (2017) 531–539. doi:10.1016/j.jallcom.2017.08.157.
- [3]. P. Mukhopadhyay, Alloy Designation, Processing, and Use of AA6XXX Series Aluminium Alloys, ISRN Metall. 2012 (2012) 1–15. doi:10.5402/2012/165082.
- [4]. B. Choudhury, M. Chandrasekaran, Investigation on welding characteristics of aerospace materials - A review, Mater. Today Proc. 4 (2017) 7519–7526. doi:10.1016/j.matpr.2017.07.083.

- [5]. R.R. Ambriz, V. Mayagoitia, I.P.N. Ciitec-ipn, Welding of Aluminum Alloys, Welding, Brazing Solder. (2018) 722–739. doi:10.31399/asm.hb.v06.a0001436.
- [6]. P.J. Modenesi, The chemistry of TIG weld bead formation, Weld. Int. 29 (2015) 771–782. doi:10.1080/09507116.2014.932990.
- [7]. A.K. Singh, V. Dey, R.N. Rai, Techniques to improve weld penetration in TIG welding (A review), Mater. Today Proc. 4 (2017) 1252–1259. doi:10.1016/j.matpr.2017.01.145.
- [8]. R.S. Vidyarthi, D.K. Dwivedi, Activating flux tungsten inert gas welding for enhanced weld penetration, J. Manuf. Process. 22 (2016) 211–228. doi:10.1016/j.jmapro.2016.03.012.
- [9]. R.S. Vidyarthi, D.K. Dwivedi, Microstructural and mechanical properties assessment of the P91 A-TIG weld joints, J. Manuf. Process. 31 (2018) 523–535. doi:10.1016/j.jmapro.2017.12.012.
- [10]. K.D. Ramkumar, V. Varma, M. Prasad, N.D. Rajan, N.S. Shanmugam, Effect of activated flux on penetration depth, microstructure and mechanical properties of Ti-6Al-4V TIG welds, J. Mater. Process. Technol. 261 (2018) 233–241. doi:10.1016/j.jmatprotec.2018.06.024.
- [11]. H. Kumar, N.K. Singh, Performance of activated TIG welding in 304 austenitic stainless steel welds, Mater. Today Proc. 4 (2017) 9914–9918. doi:10.1016/j.matpr.2017.06.293.
- [12]. R.S. Vidyarthi, A. Kulkarni, D.K. Dwivedi, Study of microstructure and mechanical property relationships of A-TIG welded P91–316L dissimilar steel joint, Mater. Sci. Eng. A. 695 (2017) 249–257. doi:10.1016/j.msea.2017.04.038.
- [13]. B. Wu, B. Wang, X. Zhao, H. Peng, Effect of active fluxes on thermophysical properties of 309L stainless-steel welds, J. Mater. Process. Technol. 255 (2018) 212–218. doi:10.1016/j.jmatprotec.2017.12.018.

Cite this article as :

Rajiv Kumar, Harmesh Kumar Kansal, S. C. Vettivel, "Experimental Investigation on Micro Structure and Mechanical Behavior of AA 6063 - 7075 Dissimilar joint using Activated TIG Welding", International Journal of Scientific Research in Science, Engineering and Technology (IJSRSET), Online ISSN : 2394-4099, Print ISSN : 2395-1990, Volume 10 Issue 1, pp. 66-73, January-February 2023.
Journal URL : <https://ijsrset.com/IJSRSET231019>